Available online at www.sciencedirect.com
ScienceDirect
Journal of Molecular Catalysis A: Chemical 259 (2006) 51–60
JOURNAL OF MOLECULAR CATALYSIS A: CHEMICAL
www.elsevier.com/locate/molcata

Sol–gel synthesis of Pt/Al_2O_3 catalysts: Effect of Pt precursor and calcination procedure on Pt dispersion

Linjie Hu, Kenneth A. Boateng, Josephine M. Hill *

Department of Chemical and Petroleum Engineering, University of Calgary, 2500 University Dr NW Calgary, Alberta T2N 1N4, Canada

Received 26 January 2006; received in revised form 31 May 2006; accepted 2 June 2006
Available online 18 July 2006

Abstract

Pt/Al_2O_3 catalysts are used in a wide variety of reactions. Tailoring the catalyst structure is important in order to efficiently and effectively utilize the noble metal. In this work, the effects of Pt precursor ($Pt(NH_3)_4Cl_2$, $Pt(C_5H_5N)_4Cl_2$, $Pt(CH_3NH_2)_4Cl_2$, or $Pt(C_4H_9NH_2)_4Cl_2$) and calcination procedure (heating rates of 2 °C/min or 10 °C/min in different atmospheres) have been investigated for 1.5 wt% Pt/Al_2O_3 catalysts prepared by sol–gel synthesis. After drying, calcination, and reduction, the Pt dispersion was measured by H_2 chemisorption. The catalyst structures were characterized using X-ray diffraction, N_2 adsorption, and transmission electron microscopy. The Pt precursors as well as the calcination procedures influenced the Pt dispersion. Higher dispersions were obtained using a lower heating rate (2 °C/min), an ammonia precursor, and a flowing gas stream (as opposed to static). Monitoring the emissions during calcination with time resolved mass spectrometry indicated that decomposition of the precursors could be achieved in helium and that subsequent treatment in oxygen was not required. Differential thermal analysis indicated that larger heat flows resulted at the higher heating rate (10 °C/min) and with the pyridine precursor, compared to the ammonia precursor. The larger heat flows may have caused more sintering and, thus, a lower dispersion. Toluene hydrogenation was used as a model reaction to demonstrate that the catalysts with higher dispersions had higher activities and better catalyst stability.

Keywords: Platinum catalyst; Alumina; Sol–gel method; Calcination; Dispersion

1. Introduction

Supported noble metal catalysts are widely used in different catalytic processes, such as petroleum refining and automotive exhaust emission control. Currently there is much interest in tailored catalyst design due to the need to produce new catalysts to meet the growing world energy demand and to develop new technologies to make more active, selective, and stable catalysts. Sol–gel synthesis is an attractive catalyst preparation method for supported noble metal catalysts [1]. This method can be used to produce catalysts with uniform metal distribution, tuneable particle size, high surface area, and stable dispersion. The technique is based on the hydrolysis of molecular precursors, mostly metal or semi-metal alkoxides. Hydrolysis and polycondensation reactions lead to the formation of oxo polymers or metal oxides. These fundamental chemical processes are influenced by several parameters which control the homogeneity and the microstructure of the derived material [2].

Supported catalysts prepared via the sol–gel method generally exhibit better thermal stability compared with carrier systems generated by impregnation and co-impregnation because of strong metal–support interactions [3–5]. For example, metal/ceramic composites have been prepared within a SiO_2 matrix that are nano-sized, non-agglomerated, and homogeneously distributed with narrow particle size distributions and adjustable metal loadings [6–8]. Zou et al. [9] studied the thermal stability of silica supported Pd catalysts prepared by the sol–gel method, and found that the Pd particles were stable at temperatures of up to 650 °C for 22 h in an O_2 atmosphere. Cho et al. [10] studied sol–gel processed Pt/Al_2O_3 with XAFS, and found the Pt particles are partially buried in the alumina. This burial of particles was the cause of a strong metal support interaction and resulted in high sintering resistance of metal particles at 600 °C in air.

* Corresponding author. Tel.: +1 403 210 9488; fax: +1 403 284 4852.
E-mail address: jhill@ucalgary.ca (J.M. Hill).

1381-1169/$ – see front matter © 2006 Elsevier B.V. All rights reserved.
doi:10.1016/j.molcata.2006.06.018

The difficulty with using sol–gel synthesis is that the catalyst properties are very sensitive to changes in the processing conditions [1,2,11–14]. During the sol–gel process, a gel forms because of the condensation of partially hydrolyzed species into a three-dimensional polymeric network. Ward and Ho [14] suggest that any factors that affect either or both of these reactions (hydrolysis and condensation) are likely to impact the final properties of the gel, and in turn, the properties of the final catalyst. These factors, as stated, include type of precursor, type of solvent, water content, acid or base content, precursor concentration, and temperature [14]. These sol–gel parameters have been extensively studied over SiO_2-based catalytic materials [1,2,11–14].

Alumina supported platinum catalysts also have been prepared using a sol–gel method [1,4,5,10,15–19]. Romero-Pascual et al. [4] studied the influence of platinum content, metal precursor, and water/alkoxide ratio on platinum particle size and thermal stability. An optimum water/alkoxide ratio was found by the researchers. The platinum particles derived from $Pt(AcAc)_2$ are larger than those from H_2PtCl_6. Khelifi and Ghorbel [11] studied the influence of hydrolysis and gelation process on thermal stability of Pt particles. Various gelation processes were performed either by the help of water, acetic acid, or by a slow condensation without a hydrolysis source. The catalyst prepared by acetic acid exhibited better sintering resistance. Few publications have been found, however, about the influence of calcination or pretreatment on the platinum dispersion for Pt/Al_2O_3. In addition, there are few studies on the effects of platinum precursors other than H_2PtCl_6 and $Pt(AcAc)_2$.

In this paper, 1.5 wt% Pt/Al_2O_3 catalysts were prepared using a single-step sol–gel method with various Pt precursors and calcination procedures. The platinum precursors include $Pt(NH_3)_4Cl_2$, $Pt(CH_3NH_2)_4Cl_2$, $Pt(C_5H_5N)_4Cl_2$, and $Pt(C_4H_9NH_2)_4Cl_2$ which all have nitrogen-containing ligands and are soluble in water. The effects of ligand in the Pt precursor, as well as the calcination procedure and atmosphere, have been investigated by a combination of catalyst characterization methods and calcination exhaust stream analysis by mass spectrometry. Specifically, the catalysts have been characterized using nitrogen physisorption, hydrogen chemisorption, X-ray diffraction, and transmission electron microscopy.

2. Experimental

2.1. Catalyst preparation

The platinum precursors were prepared by dissolving $PtCl_2$ (Sigma–Aldrich, +99% purity) in an aqueous solution of NH_3, CH_3NH_2, *n*-butylamine or pyridine. The solvent and excess ligands were removed by open dish drying in a fume hood. The resulting Pt precursors were $Pt(NH_3)_4Cl_2$, $Pt(C_5H_5N)_4Cl_2$, $Pt(CH_3NH_2)_4Cl_2$, and $Pt(C_4H_9NH_2)_4Cl_2$. The platinum content in the Pt precursors was determined using ICP-MS (Galbraith Labs Inc.). Elemental analysis for C, H, and N content in the Pt precursors were performed using a Perkin-Elmer 2400 CHN Analyzer. Proton and carbon NMR (Bruker AMX300) were also performed to confirm the identities of the groups present in the precursor using the BBI5 probe with the sample dissolved in dimethyl sulfoxide (DMSO) or deuterated chloroform ($CDCl_3$).

Pt-containing dry alumina gels were prepared using a sol–gel method similar to the procedure by Cho et al. [10]. Deionized water was mixed with aluminium tri-*sec*-butoxide (ATB) in an H_2O/ATB molar ratio of 100, and then stirred for 30 min at room temperature. Next, a 0.1 g/ml HNO_3 solution was added dropwise to the mixture, and stirred for 10 min. During the stirring the ATB decomposed resulting in a phase containing *sec*-butanol forming on top of a phase containing the sol. After separating *sec*-butanol from the mixture, additional HNO_3 solution was added to the sol until the HNO_3/Al ratio reached 0.5. Finally, the Pt precursor was added to the alumina sol, which was stirred at room temperature for 1 h, and then sonicated for 30 min. The sol was then placed in the fume hood for 48 h to allow the gel to form and the solvent water to evaporate. The dry gel was further dried at 110 °C for 12 h, and then at 200 °C for 2 h. The final material consisted of yellow cubic particles.

2.2. Catalyst calcination

For comparison, several methods of calcination were used. A portion of the dry gel was calcined by a one-step process. This dry gel was calcined at 550 °C in one of three ways: (1) in flowing oxygen for 2 h in a U-tube flow reactor heated on the outside by an electric furnace; (2) in flowing air for 2 h in the same U-tube flow reactor or (3) in static air in a muffle furnace for 2 h. In order to investigate the influence of heating rate, two ramping rates were used—2 or 10 °C/min. The other portion of the dry gel was calcined by a two-step process. The gel was first calcined at 550 °C (2 or 10 °C/min heating rate) in flowing helium for 0.5 h. After cooling to 50 °C, the flow was switched to pure oxygen. The temperature was then ramped to 550 °C at 2 or 10 °C/min and held for 2 h.

For some of the calcinations, the exhaust gas composition was monitored during the temperature ramp using a Cirrus 200 Quadrupole Mass Spectrometer system (MKS) to determine which products were being produced during the calcination.

The catalysts have been named according to the Pt precursor and the calcination treatment. For instance, Al-1 refers to a catalyst containing only alumina and calcined in oxygen at 550 °C, while Py-2 refers to a catalyst prepared with a Pt–pyridine precursor and calcined in two steps with helium first and then oxygen (see Tables 1 and 2).

2.3. Catalyst characterization

The N_2 adsorption–desorption isotherms for the catalysts were measured on an AUTOSORB-1C (Quantachrome) instrument. All samples were evacuated at 120 °C until the outgas rate was below 15 μmHg/min (or 2 Pa/min) prior to analysis. The specific surface area was calculated using the BET method. The total pore volume was determined at a relative pressure $P/P_o = 0.99$. Pore size distributions were calculated from the desorption isotherms using the Barrett, Joyner, and Halenda (BJH) method. The desorption leg of the isotherm is preferred for pore analysis because it is thermodynamically more stable than

Table 1
Properties of sol–gel alumina and Pt-containing samples before and after calcination

Sample	Pt precursor	Treatment	Surface area (m^2/g)	Pore volume (ml/g)
Al-200	Al_2O_3 only	Drying in air at 200 °C (2 h)	9.4	0.012
Al-1	Al_2O_3 only	O_2 550 °C (2 h)	281	0.35
Al-2	Al_2O_3 only	He 550 °C (0.5 h), O_2 550 °C (2 h)	254	0.30
N-200	$Pt(NH_3)_4Cl_2$	Drying in air at 200 °C (2 h)	0	–
N-1	$Pt(NH_3)_4Cl_2$	O_2 550 °C (2 h)	269	0.34
N-2	$Pt(NH_3)_4Cl_2$	He 550 °C (0.5 h), O_2 550 °C (2 h)	262	0.33
Py-200	$Pt(C_5H_5N)_4Cl_2$	Drying in air at 200 °C (2 h)	0	–
Py-1	$Pt(C_5H_5N)_4Cl_2$	O_2 550 °C (2 h)	272	0.32
Py-2	$Pt(C_5H_5N)_4Cl_2$	He 550 °C (0.5 h), O_2 550 °C (2 h)	254	0.32
Commercial γ-Al_2O_3	–	–	208	0.31

Note: Error is ±5% in the surface area and the pore volume measurements.

the adsorption leg due to the lower Gibb's free energy change [20].

H_2 chemisorption measurements were carried out on the same AUTOSORB-1C instrument. For these measurements, approximately 1.0 g of catalyst was placed in a quartz U-tube (i.d. = 10 mm), and reduced in a H_2 flow of 15 ml/min at 300 °C for 2 h. After reduction, the sample cell was evacuated at 300 °C for 2 h, and then cooled to 40 °C for the H_2 chemisorption measurement. The H_2 monolayer uptake of the catalysts was calculated by extrapolating the H_2 adsorption isotherm to zero pressure. The Pt particle diameter (d_{Pt}) was calculated using the formula, $d_{Pt} = 6V/S$, where V is the volume of total metallic Pt, and S is the active Pt surface area, assuming the Pt^{2+} ions were reduced completely and the Pt particles were spherical in shape. An adsorption stoichiometry of one hydrogen atom adsorbed per surface Pt atom ($H/Pt_s = 1$) was assumed. The percent Pt dispersion was calculated by dividing the number of exposed surface Pt atoms (as determined by H_2 chemisorption) by the total amount of Pt in the catalyst.

Powder X-ray diffraction (XRD) spectra were recorded on a Multiflex X-ray diffractometer (Rigaku) using Cu $K\alpha_1$ radiation ($\lambda = 1.54056$ Å) at 40 kV tube voltage and 40 mA tube current with a scanning speed of either 0.2 or 2°/min. The XRD patterns were referenced to the powder diffraction files (ICDD-FDP database) for identification. If possible, the average crystallite diameter of metallic Pt was calculated using Scherer's method, $D_{Pt} = K\lambda/\beta\cos\theta$, where the constant K was taken as 0.9 and β was the full width at half maximum (FWHM) of the Pt(3 1 1) peak at $2\theta = 81.3°$.

Transmission electron microscopy (TEM) images were recorded on an H-7000 transmission electron microscope (Hitachi) at 75 kV. The samples were ground to a fine powder, and mixed with acetone to make a suspension. A drop of the suspension was placed on a lacey carbon nickel grid, which was subsequently dried at room temperature before the measurement.

2.4. Differential thermal and thermogravimetric analyses

Differential thermal and thermogravimetric analyses (DTA/TGA) were performed on three samples (A1-200, N-200, and Py-200) to examine the thermal and gravimetric changes that occur in those samples during calcination. A DSC/TGA Q600 instrument (TA Instruments) was used for this analysis. The analysis conditions were selected so as to mimic the calcination procedure. Three different types of tests were performed as follows: (1) all samples (A1-200, N-200, and Py-200) were heated under air flow from room temperature to 550 °C at

Table 2
Pt dispersions of Pt/Al_2O_3 samples after various calcination procedures

Sample	Pt precursor	Calcination procedure	Heating rate (°C/min)	Pt metal content (%)	Active metal surface area (m^2/g)	Dispersion (%)	Particle diameter (nm)
N-1	$Pt(NH_3)_4Cl_2$	O_2 550 °C (2 h)	10	1.58	1.4	35	3.2
N-2	$Pt(NH_3)_4Cl_2$	He 550 °C (0.5 h), O_2 550 °C (2 h)	10	1.58	2.3	59	1.9
N-3	$Pt(NH_3)_4Cl_2$	O_2 550 °C (2 h)	2	1.58	4.1	105	1.1
N-4	$Pt(NH_3)_4Cl_2$	He 550 °C (0.5 h), O_2 550 °C (2 h)	2	1.58	4.1	104	1.1
N-5	$Pt(NH_3)_4Cl_2$	Static air in muffle furnace, 550 °C (2 h)	2	1.58	3.4	87	1.3
N-6	$Pt(NH_3)_4Cl_2$	Flowing air, 550 °C (2 h)	2	1.58	4.1	106	1.1
Py-1	$Pt(C_5H_5N)_4Cl_2$	O_2 550 °C (2 h)	10	1.43	2.2	63	1.8
Py-2	$Pt(C_5H_5N)_4Cl_2$	He 550 °C (0.5 h), O_2 550 °C (2 h)	10	1.43	2.0	56	2.0
Py-3	$Pt(C_5H_5N)_4Cl_2$	O_2 550 °C (2 h)	2	1.43	3.1	88	1.3
Py-4	$Pt(C_5H_5N)_4Cl_2$	He 550 °C (0.5 h), O_2 550 °C (2 h)	2	1.43	2.7	77	1.3
Py-5	$Pt(C_5H_5N)_4Cl_2$	Static air in muffle furnace, 550 °C (2 h)	2	1.43	2.0	58	2.0
Py-6	$Pt(C_5H_5N)_4Cl_2$	Flowing air, 550 °C (2 h)	2	1.43	3.1	89	1.3
MA-1	$Pt(CH_3NH_2)_4Cl_2$	Static air in muffle furnace, 550 °C (2 h)	2	1.54	2.2	59	1.9
BA-1	$Pt(C_4H_9NH_2)_4Cl_2$	Static air in muffle furnace, 550 °C (2 h)	2	1.19	0.34	11	9.9

Note: (1) H_2 chemisorption was performed after reducing the catalyst on line at 300 °C for 2 h in flowing H_2. (2) Error is ±5% in the dispersion measurements.

2 °C/min and held at 550 °C for 30 min; (2) sample N-200 was heated under air flow from room temperature to 550 °C at 10 °C/min and held at 550 °C for 30 min and (3) sample N-200 was heated under He flow from room temperature to 550 °C at 10 °C/min and held at 550 °C for 30 min. Heat flow, mass loss, and differential temperatures were recorded during the analyses.

2.5. Reactivity testing

Four catalyst samples, N-4, Py-4, MA-1, and BA-1 (see Table 2) were tested for reactivity in a fixed bed reactor using hydrogenation of toluene at atmospheric pressure as a model reaction. The reactor was a quartz tube with inner diameter of 7 mm. Approximately 400 mg of catalyst was used for each run. All the catalysts particles were sieved to the same size range, 90–250 μm. Reactions were conducted at temperatures between 60 and 270 °C at 30 °C intervals. A liquid hourly space velocity (LHSV) of 1 h^{-1} was used, with a H_2 to toluene volumetric ratio of 1250. The catalysts were reduced in flowing H_2 for 2 h at 300 °C and then the temperature was reduced to the reaction temperature. The reactor effluent was analyzed using a gas chromatograph (Agilent 6890) equipped with a GS-GasPro PLOT column and a flame ionization detector (FID). The reactor came to steady state after approximately 30 min on stream. The steady-state compositions were used to calculate activities. After 120 min on stream at one temperature, the temperature was increased by 30 °C. Once at 270 °C, the reactor was cooled to 60 °C and the testing and temperature cycle repeated. One complete temperature cycle between 60 and 270 °C constituted one run. Three runs were done for each of the four catalysts.

3. Results and discussion

3.1. Physical properties of catalysts

Table 1 contains the surface areas and pore volumes for catalyst samples prepared using different Pt precursors and treatment procedures. The samples Al-200, N-200, and Py-200 exhibit very low surface areas (<10 m^2/g), which indicates that aluminium hydroxide and nitrate were not decomposed to refractory oxide Al_2O_3 after being dried in air at 200 °C for 2 h. The remaining catalysts had surface areas between 254 and 281 m^2/g, and pore volumes between 0.30 and 0.35 ml/g. The pore size distributions were similar for all of the calcined catalysts, with mean pore diameters of 3.8 nm. These results indicate that the precursor and calcination procedure had little effect on the bulk physical structure of the catalysts.

For comparison, a commercial γ-Al_2O_3 (Alfa Aesar) was characterized. The surface area of the commercial alumina is slightly lower (208 m^2/g) than the surface areas of the prepared catalysts, while the pore volume is similar (Table 1). Fig. 1 compares the pore size distributions and adsorption isotherms of the commercial alumina and sample Al-1, which is representative of all the calcined catalysts. The in-house prepared alumina is similar to the commercial alumina in terms of its pore structure.

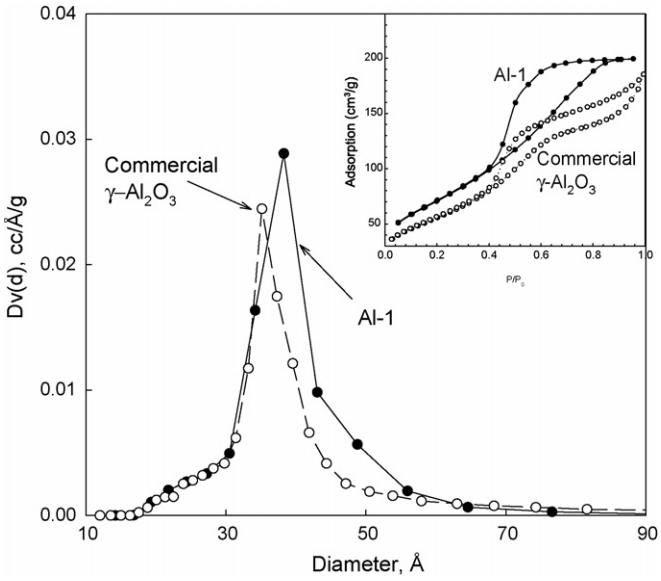

Fig. 1. Pore size distributions and adsorption isotherms of samples Al-1 and commercial γ-Al_2O_3 (Alfa Aesar). Sample Al-1 is representative of all in-house prepared samples with or without platinum.

Based on the elemental analysis performed by ICP-MS (Galbraith Labs), the platinum content of the catalysts are as follows: 1.58% for N-batch catalysts, 1.43% for Py-batch samples, 1.54% for MA-1, and 1.19% for BA-1. These Pt metal contents are shown in Table 2, with the Pt dispersions as determined by H_2 chemisorption. The dispersions range between 11 and 106%. The metal surface areas used to calculate the dispersions are also shown in Table 2. Dispersions above 100% may be attributed to errors in the Pt metal content, errors in the adsorbed H_2 determination, or hydrogen spillover from the Pt. The Autosorb-1C was calibrated with the Quantachrome standard reference (1%Pt/Al_2O_3), and had an error of ±0.5%.

In general, a lower heating rate (2 °C/min versus 10 °C/min) results in an increased dispersion. In addition, the precursor may also significantly influence the dispersion, as will be discussed in more detail in the following sections. In this work, all comparisons are made between the same batches of catalyst. Despite batch to batch variability, the overall trends are consistent.

The diameter of the Pt particles can be estimated from the hydrogen uptake and is given in Table 2. For all catalysts, except BA-1, the average particle sizes of Pt are less than 3.2 nm. X-ray diffraction can also be used to estimate the particle size provided that the particles are larger than approximately 4–5 nm. Fig. 2 shows the XRD spectra of the prepared catalysts and a commercial γ-Al_2O_3. The XRD pattern of aluminium oxide can be quite different depending on the preparation method and crystalline phase according to the ICDD-FDP database. The spectra in Fig. 2 indicate that the commercial γ-Al_2O_3 sample and the in-house prepared samples have similar structures although the latter alumina has smaller crystalline size as indicated by the broader peaks at $2\theta = 67.3°$. The XRD patterns of the samples are all quite similar despite different platinum particle sizes, calcination procedures, and platinum precursors. This result indicates that the alumina crystalline structure is not sensitive to these

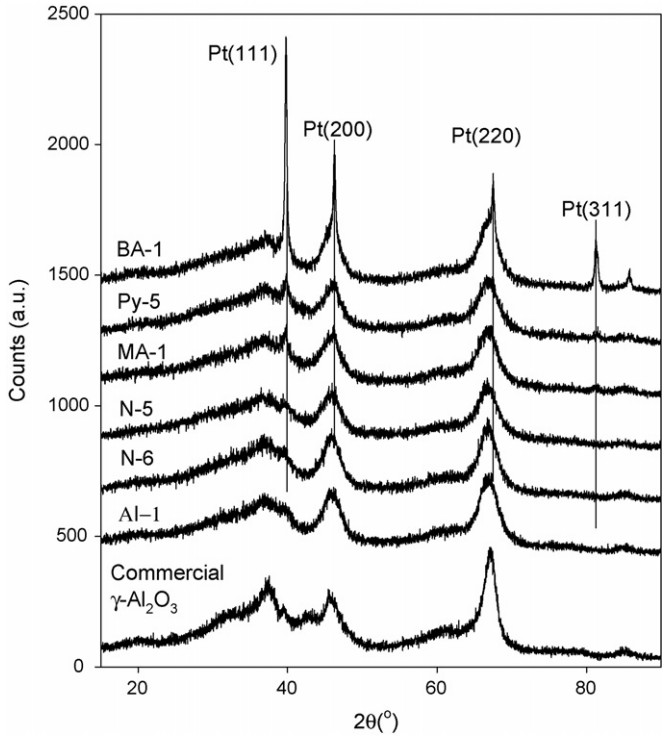

Fig. 2. XRD patterns of alumina samples and Pt/Al_2O_3 catalysts. All samples were calcined. Catalysts were reduced at 300 °C for 2 h with flowing H_2.

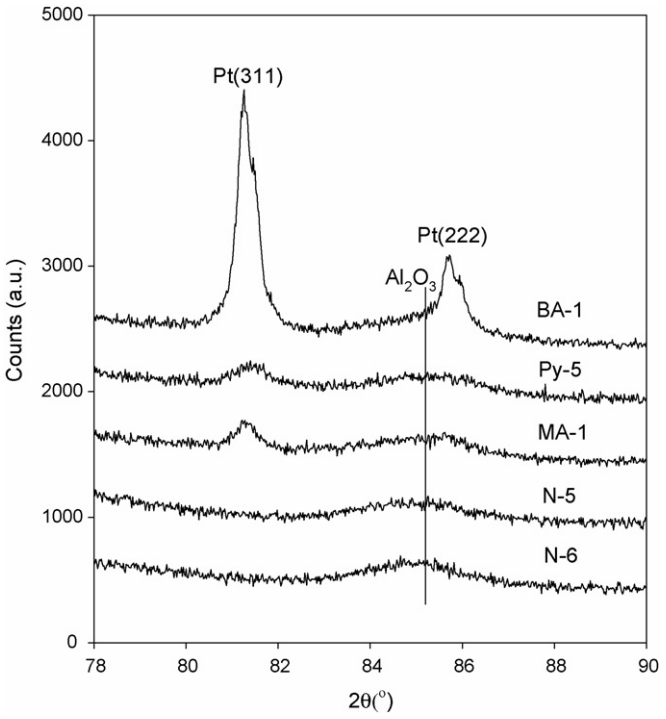

Fig. 3. XRD patterns of reduced Pt/Al_2O_3 catalysts obtained with slow scans (0.2°/min).

parameters, which is consistent with the BET measurements with respect to the constant pore structure and surface area.

The peaks for Pt overlap, at least partially, with alumina at most diffraction angles, except for the Pt(3 1 1) peak at $2\theta = 81.3°$. In order to obtain accurate Pt particle size information, slow scans (0.2°/min) were performed in the range of 78–90° 2θ. The results are shown in Fig. 3 and are consistent with the average particle size of Pt calculated from the chemisorption results. Pt is undetectable for catalysts N-5 and N-6, while Py-5 and MA-1 both have a peak at $2\theta = 81.3°$ that is too small for estimation of particle size. The calculated average particle size of Pt in catalyst BA-1 is 23 nm, which is larger than that estimated by hydrogen chemisorption (10 nm).

3.2. Effect of platinum precursor

The platinum precursors – $Pt(NH_3)_4Cl_2$, $Pt(CH_3NH_2)_4Cl_2$, $Pt(C_5H_5N)_4Cl_2$, and $Pt(C_4H_9NH_2)_4Cl_2$ – were analyzed with CHN analysis to obtain the C, H, and N ratios contained in the catalysts. Based on the CHN analysis results, it was confirmed that the desired precursors were obtained. Carbon NMR of the $Pt(C_4H_9NH_2)_4Cl_2$ precursor showed a CH_3 chemical shift at 13.7 ppm and CH_2 at 19.4, 32.7, and 46.1 ppm. Proton NMR of the same $Pt(C_4H_9NH_2)_4Cl_2$ confirmed the presence of the CH_3 and CH_2 peaks in addition to the NH_2 peak at ca. 5.6 ppm chemical shift. These results in addition to the CHN analysis confirmed the presence of a ($C_4H_9NH_2$) group in the precursor. Proton NMR of the $Pt(C_5H_5N)_4Cl_2$ precursor revealed an aromatic structure with the first CH at 8.9 ppm, the second at 7.5 ppm, and the third at 7.9 ppm. Combined with results of CHN analysis, these results confirmed the presence of a (C_5H_5N) group in the precursor.

The selection of platinum precursor was based on the hypothesis that the larger the precursor the better the resulting Pt dispersion. During calcination, platinum (oxide) atoms may agglomerate into clusters. Assuming that the agglomeration occurs as a series of binary interactions, the rate of agglomeration is related to the distance between any two platinum atoms. Thus, the ligand of the Pt(II) precursor would act as space holder for the platinum atoms. As shown in Table 2, the precursors are all nitrogen-containing molecules and soluble in water. The molecular diameters of the precursors were estimated by bond lengths and are approximately 5, 7, 12, and 13 Å for $Pt(NH_3)_4Cl_2$, $Pt(CH_3NH_2)_4Cl_2$, $Pt(C_5H_5N)_4Cl_2$, and $Pt(C_4H_9NH_2)_4Cl_2$, respectively.

Fig. 4 illustrates that the results were exactly the opposite of what was expected. That is, the smaller the precursor, the better the dispersion. The results shown in Fig. 4 are those taken from Table 2 for samples N-5, Py-5, MA-1, and BA-1. The Pt dispersion is strongly dependent on the precursor and increases from 11% for BA-1 (largest precursor) to 87% for N-5 (smallest precursor). These samples were calcined in a muffle furnace in static air. Although, as discussed below, calcining in static air results in lower dispersions than flowing air, the trend of increasing dispersion with decreasing precursor size did not change with a change in the calcination procedure.

The extremely low dispersion of BA-1, obtained using $Pt(C_4H_9NH_2)_4Cl_2$ as precursor, may be caused partly by the relatively poor solubility of the precursor in water. During the precursor preparation, the water solution (15 ml water, contain-

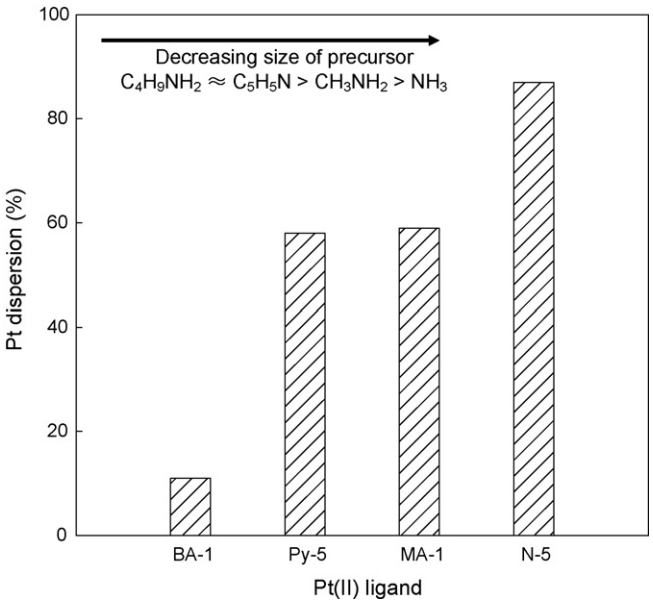

Fig. 4. Influence of platinum precursors on dispersion in Pt/Al_2O_3 catalysts. The dry gels were calcined in a muffle furnace at 550 °C for 2 h with a heating rate of 2 °C/min, and reduced at 300 °C for 2 h in flowing H_2.

ing 0.1 g of Pt) had to be heated to 60 °C in order to dissolve this precursor. The precursor did not precipitate in the sol or wet gel because of the presence of sufficient water (ca. 50 ml). The precursor, $Pt(C_4H_9NH_2)_4Cl_2$, probably precipitated, however, during water removal. If the precipitate separated from the alumina gel during subsequent heat treatments, large Pt particles may be formed. TEM analysis of the reduced BA-1 catalyst (Fig. 5) indicated that large Pt particles have formed. The darker particles in Fig. 5(a) are on the order of 200 nm in size and are likely Pt particles or agglomerates. The lighter particles are alumina. In Fig. 5(b), Pt particles are visible at the edges of the alumina particles with sizes of 10–50 nm. A homogenous Pt distribution was not obtained from this Pt precursor as the majority of the alumina particles did not contain any visible Pt particles. On all other catalysts, no Pt particles were visible, consistent with the hydrogen chemisorption and XRD results.

The chemical nature of the Pt precursors and their interaction with the support precursor (i.e., silane as precursor of silica) may also be a factor in the resulting metal dispersion. The effect of Pt precursor on the Pt dispersion and particle size has been studied over sol–gel processed Pt/SiO_2 by Lembacher [2]. The studied precursors included $Pt(AcAc)_2$, $PtCl_2$, H_2PtCl_6, Na_2PtCl_6, $Pt(CN)_2$, and $Pt(NH_3)_4(NO_3)_2$. $PtCl_2$ led to the highest Pt dispersion when a nitrogen-containing silane, $H_2NCH_2CH_2NH(CH_2)_3Si(OEt)_3$ (AEAPTS), was used as silica precursor. The researchers ascribed this result to the strong interaction of Pt(II) and the silica precursor, while Pt(IV) cannot form a complex with nitrogen-containing molecules with a silica precursor. In the work done herein, the Pt precursors will not react with the aluminium precursors and so anchoring of some of the Pt precursors cannot explain the different dispersions that were obtained.

3.3. The effect of calcination procedure on Pt dispersion

A heating rate of 2 °C/min under all calcination conditions resulted in higher Pt dispersions than using a heating rate of 10 °C/min. Fig. 6 presents the results for the catalysts derived from $Pt(NH_3)_4Cl_2$. Samples N-1 (35% dispersion) and N-3 (105% dispersion) were both calcined in O_2 at 550 °C for 2 h, while samples N-2 (59% dispersion) and N-4 (104% dispersion) were calcined in a two-step process involving helium and then oxygen. Clearly a slower heating rate results in higher dispersions. The same trend is observed for the catalysts prepared with $Pt(C_5H_5N)_4Cl_2$ as the precursor (Py-catalysts). For example, the Pt dispersion for Py-3, heated at 2 °C/min, was 88%, compared to a Pt dispersion of 63% for Py-1, which was heated at 10 °C/min. We have not found any literature demonstrating that a slower heating rate is better for the preparation of Pt/Al_2O_3 catalysts, although this result is expected based on the results for silica-supported catalysts.

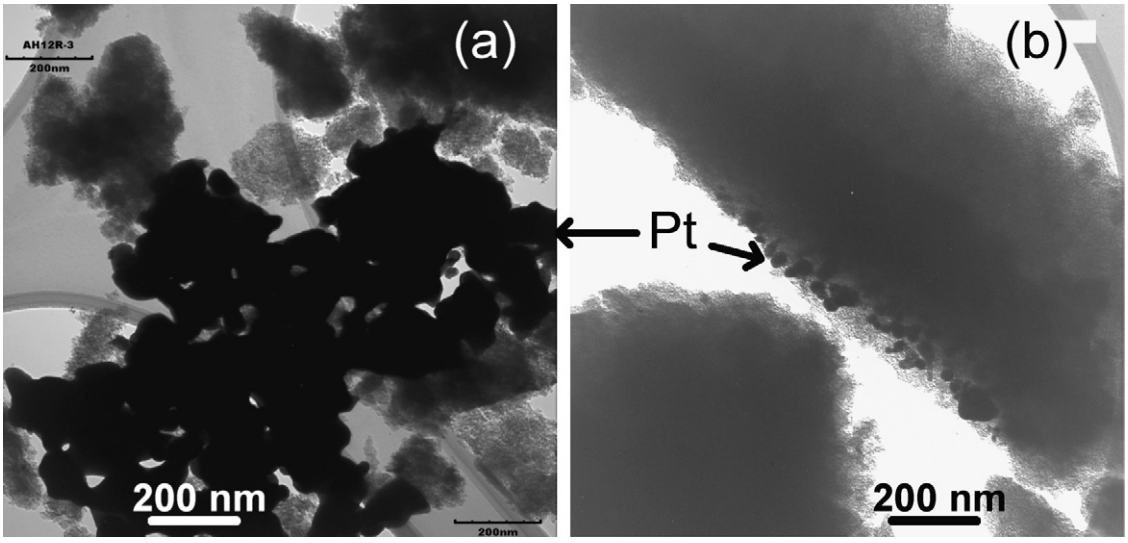

Fig. 5. (a and b) TEM images of catalyst BA-1.

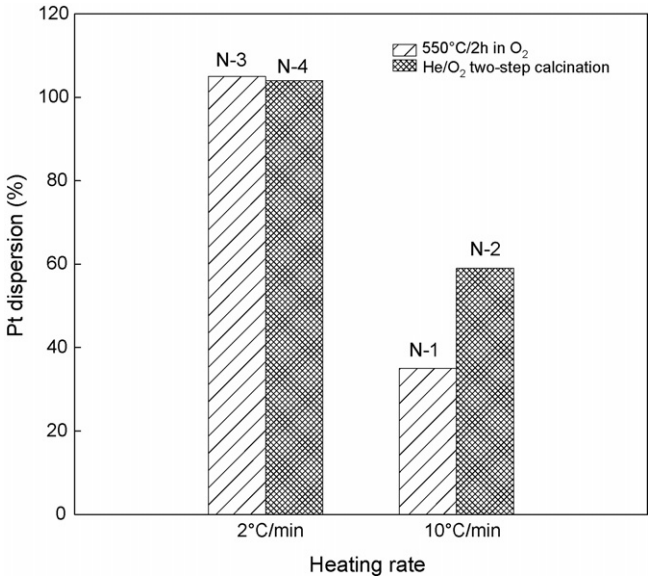

Fig. 6. Influence of heating rate during calcination on Pt dispersion of Pt/Al_2O_3 catalysts. The dry gel was calcined in flowing gas at a heating rate of 2 or 10 °C/min.

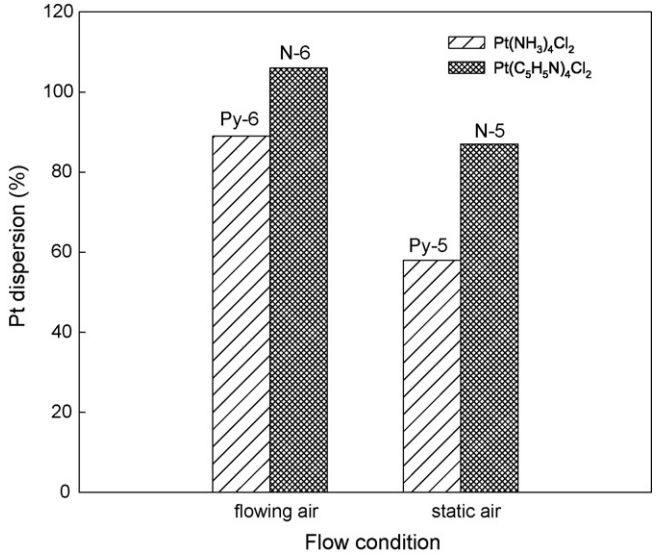

Fig. 7. Influence of gas flow during calcination on Pt dispersion of Pt/Al_2O_3 catalysts. All the catalysts were calcined either in flowing air or in static air (muffle furnace) at a heating rate of 2 °C/min.

The atmosphere during calcination also affected the final Pt dispersion, but the magnitude of the effect depended on the heating rate and Pt precursor. For example, samples N-1 and N-2, were both prepared from the same precursor and heated at the same rate (10 °C/min) during calcination, but had significantly different Pt dispersions (35% versus 59%). In this case, a higher dispersion was obtained by heating in He before heating in O_2. Conversely, for samples N-3 and N-4 (Table 2), heated at 2 °C/min, the Pt dispersion was the same regardless of the calcination procedure. When $Pt(C_5H_5N)_4Cl_2$ was used as the Pt precursor, a comparison of Py-1 with Py-2, and Py-3 with Py-4 (Table 2), indicated that He pretreatment before calcination in O_2 resulted in a lower Pt dispersion compared to no He pretreatment. Lembacher has shown that pretreatment in an inert atmosphere is beneficial for Pt dispersion on silica supports [2]. For Pt/SiO_2 the average particle size of Pt decreased from 22 nm to less than 3 nm by pretreating the catalyst with argon before exposure to air at 400 °C [2]. The author suggested that, during the one-step calcination, the Pt particles sintered due to local overheating caused by rapid oxidation of organic groups in the silane precursor. It is unclear, however, how the organic groups in the metal precursors affect the dispersion during calcination.

Heating in a muffle furnace is a much simpler method than heating a catalyst in a flow apparatus. In these experiments, however, treatment in static air (i.e., the muffle furnace) resulted in much lower Pt dispersions than treatment in a U-tube on a flow apparatus. For example, as shown in Fig. 7 and Table 2, sample N-5 was calcined in the muffle furnace and had a Pt dispersion of 87% compared to a dispersion of 106% for sample N-6, calcined in flowing air. Similar results were obtained for samples Py-5 and Py-6. Likely the water produced during the calcination was not removed quickly enough without flowing gases. The presence of water may have promoted the sintering of the Pt particles [15,21,22].

3.4. Calcination studies performed by mass spectrometry

Mass spectrometry (MS) was used to better understand what species are being formed during the calcination. This analysis was used in conjunction with XRD analysis. The alumina support was analyzed first, and then several samples containing Pt were analyzed. The alumina gel is soluble in water after drying at 200 °C for 2 h, indicating the dry gel has the same or similar composition with the sol or wet gel except for solvent (H_2O) content. In order to investigate the structure of the dry gel (Al-200 in Table 2), the XRD patterns were recorded before and after calcinations (spectra not shown). The XRD pattern of the dry gel was different from that of the sol–gel Al_2O_3 (Al-1 and Al-2). Referencing the ICDD database, the dry gel had a similar structure to $Al(OH)_3$, indicating the dry gel did not decompose after drying for 2 h at 200 °C in air. The composition of the dry gel can be represented by $Al(NO_3)_\delta(OH)_{3-\delta}$, or more precisely $Al(NO_3)_\delta O_x(OH)_{3-\delta-2x}$ because of condensation [23]. Here, $\delta \approx 0.5$ since the molar ratio of HNO_3/Al is 0.5 during peptization. After calcination, the mass loss of the dry gel is $45 \pm 4\%$. From the mass loss, the value of x can be calculated, which will be discussed in Section 3.5. The calcined alumina samples (Al-1 and Al-2) had structures similar to a commercial γ-Al_2O_3 as described previously.

Fig. 8 shows the evolution of CO_2 (mass 44) and NO_2 (mass 46) during the calcination of the dry gel in oxygen or in helium. Masses 18 (H_2O) and 30 were also monitored during the experiment. During calcination water was produced from the decomposition of $Al(OH)_3$. The water, however, condensed before the inlet to the mass spectrometer and, thus, the water signal is not reliable and not shown. The signals from masses 46 and 30 were identical in shape and, thus, mass 30 is attributed to the cracking pattern of NO_2 [24]. The plots in Fig. 8 are nearly identical whether the atmosphere is helium or oxygen. In both cases, CO_2 is detected at temperatures between 240 and 470 °C, while NO_2

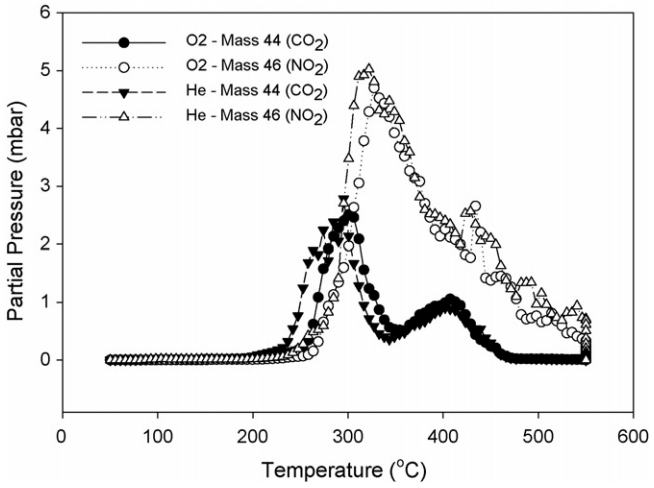

Fig. 8. CO_2 and NO_2 evolution monitored by mass spectrometry during calcination of dry gel alumina (Al-200) in flowing O_2 or He (20 ml/min, 10 °C/min).

is detected at temperatures above 250 °C. The CO_2 originated from the oxidation of an organic compound in the gel produced during the hydrolysis of ATB. The organic compound is likely 2-butanol; however, 2-butanol was not detected in the emissions. The organics were oxidized by oxygen or the produced NO_x in the absence of oxygen (i.e., helium atmosphere). Following the treatment in flowing He, the same sample was monitored during treatment in flowing O_2 and no NO_2 or CO_2 was detected. These results suggest that complete decomposition occurred during the pre-treatment in helium and that treatment with oxygen was unnecessary.

The NO_2, NO, and H_2O emissions during the calcination of Pt-containing dry gels (N-200 and Py-200) were similar to that for blank alumina gel (Al-200) in either oxygen or helium. The CO_2 evolution during the calcination of Al-200, N-200, and Py-200 is shown in Fig. 9. The plots are similar for a

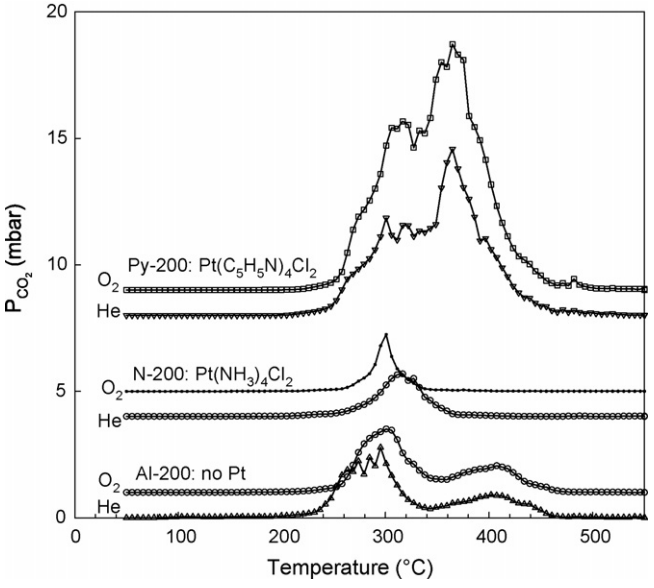

Fig. 9. CO_2 evolution monitored by mass spectrometry during calcination of Al-200, N-200, and Py-200 in flowing O_2 or He (20 ml/min, 10 °C/min).

helium or oxygen atmosphere. The quantity of CO_2 evolved, however, depended on the presence of the precursor. Emissions of CO_2 for the gel derived from $Pt(NH_3)_4Cl_2$ (N-200) and for a blank alumina gel (Al-200) were similar. In comparison, the gel derived from $Pt(C_5H_5N)_4Cl_2$ (Py-200) produced approximately 20 times more CO_2 than either N-200 or Al-200, consistent with the carbon content of the precursor. The additional emitted CO_2 came from the oxidation of the pyridine contained in the dry gel for Py-200.

3.5. Chemical reactions during calcination

As mentioned above, the composition of the alumina dry gel before calcination can be represented by $Al(NO_3)_\delta O_x(OH)_{3-\delta-2x}$, $\delta \approx 0.5$. The value of x can then be calculated based on mass loss during calcination. The final solid product after calcination is Al_2O_3, and the mass losses are $45 \pm 4\%$ during calcination. Thus, the reaction during calcination can be described as follows:

$$2Al(NO_3)_{0.5}O_x(OH)_{2.5-2x} = Al_2O_3 + NO_2 + (2.5-2x)H_2O + 0.25O_2 \quad (1)$$

The calculated value of x is between 0 and ~0.8. On average, if the mass loss is 45%, $x \approx 0.4$. That is, 100 g of the dry gel would produce 25 g of NO_2, 4.3 g of O_2, and 16 g of H_2O. Water condensation in the lines after the calcination vessel was evident. The condensed water had a yellow color and was strongly acidic (pH < 1), indicating that HNO_3 likely has been formed from the following reactions in the exit stream:

$$4NO_2 + O_2 + 2H_2O = 4HNO_3 \quad (2)$$

$$3NO_2 + H_2O = NO + 2HNO_3 \quad (3)$$

Water vapor has been reported to enhance Pt sintering in Pt/Al_2O_3 during calcination and reduction [15,21,22]. The presence of excess water vapor may have been a factor in the lower dispersions obtained when the calcination was performed in static air (muffle furnace) rather than flowing air, in which the water would have been removed and not accumulated on the surface of the catalyst. Similarly, the lower heating rate (2 °C/min) may be beneficial because of the slower decomposition, and hence water evolution, of the alumina gel. The gas flow rate and amount of catalyst was kept constant throughout the calcination tests.

The effect of the Pt precursor on dispersion may be related to the composition of the precursor. In this work, the Pt precursors with organic ligands yielded lower Pt dispersions than the precursor containing ammonia. The dry gel containing a pyridine Pt(II) ligand (Py-200) produces approximately 20 times the amount of CO_2 during calcination than the dry gel containing an ammonia Pt(II) ligand (N-200). The localized heating from the oxidation of the organic ligands may have been sufficient to result in sintering of the Pt particles. Lembacher [2] suggested that localized heating caused by rapid oxidation of the support precursor, silane, resulted in sintering in Pt/SiO_2 catalysts. In contrast to the work on Pt/SiO_2 [2], with Pt/Al_2O_3 He treat-

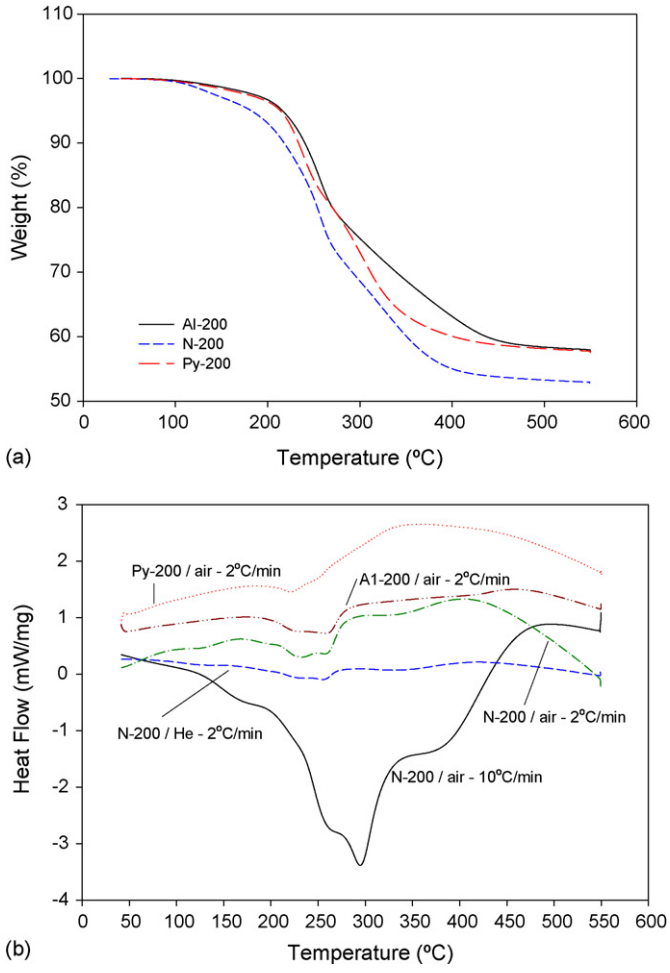

Fig. 10. Thermogravimetric (a) and differential thermal analysis (b) of A1-200, N-200, and Py-200 heated at 2 °C/min in air. The differential thermal analysis is also shown for N-200 heated at 2 °C/min in He, and at 10 °C/min in air.

ments before calcination in oxygen only improved the dispersion for the ammonia precursor with a heating rate of 10 °C/min. The mass spectrometer results indicated that the pyridine and ammonia precursors were completely oxidized in He and a second treatment in O_2 was not required. The decomposition of NO_3^- groups produced significant amounts of O_2 and NO_x which can act as oxidants. Likely these species were sufficient to completely decompose the precursors.

3.6. Results of differential thermal and thermogravimetric analyses

The thermogravimetric and differential thermal analysis of samples Al-200, N-200, and Py-200 are shown in Fig. 10. In agreement with the mass spectrometry results, the mass loss in an air atmosphere corresponded to decomposition within the temperature range of 200–450 °C (Fig. 10(a)). The differential thermal analysis is shown for two heating rates (2 and 10 °C/min) as well as two atmospheres (helium and air) for sample N-200. More heat was evolved during the calcination of Py-200 (comparable to Py-3 with a dispersion of 88%) than for the calcination of N-200 (comparable to N-3 with a dispersion of 105%). The

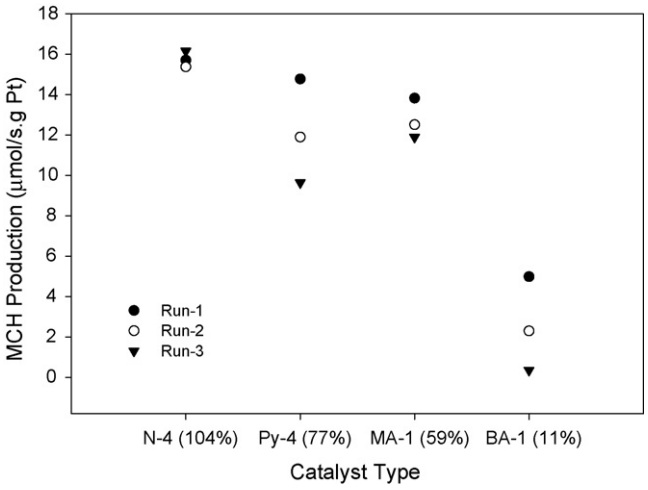

Fig. 11. Toluene hydrogenation activity of N-4, Py-4, MA-1, and BA-1 catalysts at 240 °C for three different runs: (●) run 1, (○) run 2, and (▼) run 3. The numbers given in brackets on the *x*-axis are the Pt dispersions of each catalyst.

largest change in heat flow occurred on sample N-200 heated in air at 10 °C/min, which is consistent with the lower dispersions obtained for samples heated at 10 °C/min than 2 °C/min (Table 2). These results support the theory that localized heating during calcination may contribute to sintering of the Pt resulting in lower dispersions.

3.7. Reactivity tests—toluene hydrogenation

Fig. 11 shows a comparison of the production of methylcyclohexane (MCH) over catalysts produced from the different precursors (N-4, Py-4, MA-1, and BA-1) at 240 °C and atmospheric pressure. Three runs were performed for each catalyst and in each case, the only product was methylcyclohexane. Catalyst BA-1 had the lowest Pt dispersion (11%) and the lowest production of MCH. In contrast, catalyst N-4 had the highest Pt dispersion (104%) and the highest production rate. Catalysts Py-4 and MA-1 had intermediate Pt dispersions (77 and 59%) and intermediate activities. The activity of N-4 stayed within 2.5% of the mean activity of this catalyst. The other catalysts, however, had larger decreases in activity over time.

4. Conclusions

Pt dispersions ranging between 11 and 106% were obtained for 1.5 wt% Pt/Al_2O_3 catalysts prepared by sol–gel synthesis. The Pt dispersion of the catalyst was found to be strongly dependent on the platinum precursor, and contrary to our expectation, a larger precursor molecule did not result in better dispersion. Specifically, in terms of highest Pt dispersion, $Pt(NH_3)_4Cl_2$ was the best precursor followed by $Pt(CH_3NH_2)_4Cl_2$, $Pt(C_5H_5N)_4Cl_2$, and finally $Pt(C_4H_9NH_2)_4Cl_2$. The latter precursor resulted in a very poor dispersion, likely because of its poor solubility. The dispersion also depended on the calcination procedure. The use of flowing gas instead of static air, and a lower heating rate (2 °C/min rather than 10 °C/min) resulted in higher Pt dispersions. The presence

of accumulated water (from treatment in static air or from too high a heating rate) and/or localized heating effects (dependent on the decomposition of the precursor) resulted in sintering of the Pt and lower dispersions. Pretreatment in helium before oxygen did not improve the dispersion. Toluene hydrogenation experiments indicated that higher activities and selectivities can be achieved with catalysts containing more highly dispersed Pt. Thus, it is desirable to optimize catalyst preparation to achieve high dispersion.

Acknowledgements

We would like to acknowledge Suncor Energy Inc., Alberta Energy Research Institute, and the Natural Sciences and Engineering Research Council (NSERC) for funding this project. We thank Mr. R. Humphrey and Mr. W. Dong at the Microscopy and Imaging Facility, University of Calgary, for assistance with electron microscopy, Ms. L. Klatzel-Mudry at the Department of Geology and Geophysics, University of Calgary, for assistance with XRD analysis, Ms. Q. Wu of the Chemical Instrumentation Lab at the Department of Chemistry, University of Calgary, for assistance with NMR and elemental analysis, Dr. A. Hassan for his assistance with preparing platinum precursors, and Drs. J. Perez-Zurita and A. Mahmoudkhani for performing DTA analysis.

References

[1] K. Balakrishnan, R.D. Gonzalez, J. Catal. 144 (1993) 395–413.
[2] C.U.S. Lembacher, New J. Chem. 22 (1998) 721–724.
[3] T. Ueckert, R. Lamber, N.I. Jaeger, U. Schubert, Appl. Catal. A: Gen. 155 (1997) 75–85.
[4] E. Romero-Pascual, A. Larrea, A. Monzon, R.D. Gonzalez, J. Solid State Chem. 168 (2002) 343–353.
[5] L. Khelifi, A. Ghorbel, E. Garbowski, M. Primet, J. Chimie Phys. Phys.-Chim. Biol. 94 (1997) 2016–2026.
[6] A. Kaiser, C. Görsmann, U. Schubert, J. Sol-Gel Sci. Technol. 8 (1997) 795–799.
[7] U. Schubert, S. Tewinkel, R. Lamber, Chem. Mater. 8 (1996) 2047–2055.
[8] W. Morke, R. Lamber, U. Schubert, B. Breitscheidel, Chem. Mater. 6 (1994) 1659–1666.
[9] W.Q. Zou, R.D. Gonzalez, Appl. Catal. A: Gen. 126 (1995) 351.
[10] I.H. Cho, S.B. Park, S.J. Cho, R. Ryoo, J. Catal. 173 (1998) 295–303.
[11] L. Khelifi, A. Ghorbel, J. Sol-Gel Sci. Technol. 19 (2000) 643–646.
[12] S. Fessi, A. Ghorbel, J. Sol-Gel Sci. Technol. 26 (2003) 837–841.
[13] R.D. Gonzalez, T. Lopez, R. Gomez, Catal. Today 35 (1997) 293–317.
[14] D.A. Ward, E.I. Ho, Ind. Eng. Chem. Res. 34 (1995) 421–433.
[15] T.F. Garetto, C.R. Apesteguia, Catal. Today 62 (2000) 189–199.
[16] L. Khelifi, A. Ghorbel, J. Sol-Gel Sci. Technol. 26 (2003) 847–852.
[17] E. Marceau, H. Lauron-Pernot, M. Che, J. Catal. 197 (2001) 394–405.
[18] S. Rezgui, R. Jentoft, B.C. Gates, J. Catal. 163 (1996) 496–500.
[19] E. Seker, E. Gulari, J. Catal. 194 (2000) 4–13.
[20] S. Lowell, J.E. Shields, Powder Surface Area and Porosity, third ed., Chapman and Hall, 1991.
[21] R. Prestvik, K. Moljord, K. Grande, A. Holmen, J. Catal. 174 (1998) 119–129.
[22] T.F. Garetto, C.R. Apesteguia, Appl. Catal. B: Environ. 32 (2001) 83–94.
[23] C.J. Brinker, G.W. Scherer, Sol–gel Science: The Physics and Chemistry of Sol–Gel Processing, Academic Press Inc., 1990.
[24] NIST Chemistry WebBook, NIST Standard Reference Database Number 69, June 2005 Release, http://webbook.nist.gov/cgi/cbook.cgi?Formula=NO2&NoIon=on&Units=SI&cMS=on#Mass-Spec.